Original Article
OBESITY BIOLOGY AND INTEGRATED PHYSIOLOGY

Obesity

The Vitamin K Epoxide Reductase *Vkorc1l1* Promotes Preadipocyte Differentiation in Mice

Yi Ding [1], Jing Cui [1], Qi Wang [2], Suqin Shen [3], Tian Xu [1,4], Huiru Tang [1], Min Han [1,5], and Xiaohui Wu [1]

Objective: Identification of novel regulators involved in adipose development is important to understand the molecular mechanism underlying obesity and associated metabolic disorders. Through isolation and analysis of a vitamin K epoxide reductase *Vkorc1l1* mutant, this study aimed to disclose its function and underlying mechanism in adipose development and to obtain valuable insights regarding the mechanism of obesity.

Methods: A *Vkorc1l1* mutation recovered from a forward genetic screen for obesity-related loci in mice was characterized to explore its effects in gene expression, animal metabolism, and adipose development. Adipogenesis was evaluated in both *Vkorc1l1* mutant stromal vascular fraction and *Vkorc1l1* knockdown preadipocytes. Intracellular vitamin K_2 level and the effect of vitamin K_2 on adipogenesis were tested in primary preadipocytes.

Results: *Vkorc1l1* mutants displayed a considerably lower fat to body weight ratio, substantially decreased plasma leptin, and significantly underdeveloped white adipose tissue. Adipogenic defects related with *Vkorc1l1* deficiency were observed both *in vivo* and *in vitro*. Vitamin K_2 could inhibit adipogenesis in stromal vascular fraction. Increased intracellular vitamin K_2 level was detected in *Vkorc1l1* mutant preadipocytes.

Conclusions: *Vkorc1l1* promotes adipogenesis and possibly obesity. Downregulation of *Vkorc1l1* increases intracellular vitamin K_2 level and impedes preadipocyte differentiation.

Obesity (2018) **00**, 00–00. doi:10.1002/oby.22206

Introduction

The accumulation of extra adipose tissue is one of the most characteristic features of obesity. It occurs through both enlargement of adipocyte size (hypertrophy) and increase of adipocyte number (hyperplasia) (1). In mammals, the brown adipose tissue (BAT) and white adipose tissue (WAT) are the two major types of adipose tissue. BAT is the site for thermogenesis and energy expenditure, while WAT is the major site for energy storage. Extensive cold exposure may stimulate the expression of *UCP1* and other thermogenic genes in some WAT cells, which converts these cells to the beige adipocytes (2). In mice, BAT development initiates around embryonic days 15 and 16 (E15-E16) (3), while WAT develops later. The development of subcutaneous WAT starts around E17.5 to E18.5, followed by rapid lipid accumulation in adipocytes after birth (4). Perigonadal WAT (pgWAT) develops after birth and starts accumulating lipid at the age of day 7 (P7) (5). The adipogenic process also takes place in the adult stage. In particular, high-fat diet (HFD)-induced adipogenesis has been well characterized by lineage-tracing experiments in adult mice (6). Approximately 5% of adipocytes are replaced daily in adult mice (7). In adult humans, the turnover rate is approximately 10% per year (8).

White adipocytes are differentiated from preadipocytes in a process known as adipogenesis. Most preadipocytes are originated from cells

[1] State Key Laboratory of Genetic Engineering and National Center for International Research of Development and Disease, Institute of Developmental Biology and Molecular Medicine, Collaborative Innovation Center of Genetics and Development, School of Life Sciences, Fudan University, Shanghai, China. Correspondence: Xiaohui Wu (xiaohui_wu@fudan.edu.cn) [2] Key Laboratory of Magnetic Resonance in Biological Systems, State Key Laboratory of Magnetic Resonance and Atomic and Molecular Physics, National Centre for Magnetic Resonance, Wuhan Institute of Physics and Mathematics, University of Chinese Academy of Sciences, Wuhan, China [3] State Key Laboratory of Genetic Engineering, School of Life Sciences, Fudan University, Shanghai, China [4] Department of Genetics, Howard Hughes Medical Institute, Yale University School of Medicine, New Haven, Connecticut, USA [5] Department of Molecular, Cellular, and Developmental Biology, Howard Hughes Medical Institute, University of Colorado, Boulder, Colorado, USA.

Funding agencies: This work was supported in part by National Natural Science Foundation of China Grant 81570756 and Shanghai Municipal Science and Technology Commission Grant 15XD1500500.

Disclosure: The authors declared no conflict of interest.

Author contributions: YD designed the studies, performed experiments, analyzed data, and wrote the manuscript. JC performed experiments. QW and HT performed and supervised the high-performance liquid chromatography experiments, respectively. SS supervised fluorescence activated cell sorting experiments. MH and TX supervised the work. XW conceived of and designed the studies, supervised the work, and wrote the manuscript.

Additional Supporting Information may be found in the online version of this article.

Received: 7 October 2017; **Accepted:** 16 April 2018; **Published online 00 Month 2018. doi:10.1002/oby.22206**

residing in adipose stromal vascular regions (9,10). During adipogenesis, they undergo morphological and functional change from spindle-shaped fibroblast-like cells into round and lipid-laden adipocytes (11). Bone-marrow-derived cells (BMDCs) serve as another source of adipocytes (12,13). However, the contribution of the hematopoietic lineage to the whole preadipocyte pool is fairly low and also displays a gender-specific pattern. The contribution of BMDCs in females is fourfold that in males (13).

Vitamin K is a group of fat-soluble vitamins that includes the following two natural vitamers: vitamin K_1 and vitamin K_2. Vitamin K_1 exists primarily in green leafy vegetables and can be converted to menaquinone-4, a major form of vitamin K_2, in mammal tissues (14,15). Vitamin Ks are well known for their roles in blood coagulation and bone health because of their functions in carboxylating certain glutamate residues in coagulation factors and bone proteins (14). Vitamin K deficiency caused by intestinal injury or genetic disorders may lead to severe bleeding and death (16,17). In anticoagulated patients, genetic polymorphisms related to vitamin K homeostasis are associated with hemorrhagic risks (18). Although vitamin K_1 and K_2 share similar structures and are generally considered to have similar physiological functions, experimental evidence has also suggested the functional specificities associated with each. For example, the phosphorylation of protein kinase A (PKA) could be induced by vitamin K_2 but not vitamin K_1 (19). Similarly, only vitamin K_2 could bind to the steroid and xenobiotic receptor (20).

Vitamin K homeostasis is maintained by the vitamin K recycling that converts vitamin K epoxide to vitamin K and further to vitamin K hydroquinone (21). These processes could be catalyzed by both vitamin K epoxide reductase complex subunit 1 (Vkorc1) and its paralogue vitamin K epoxide reductase complex subunit 1 like 1 (Vkorc1l1). Vkorc1 is apparently more effective in the first step, while Vkorc1l1 works more efficiently for the second (22). As expected, disruption of Vkorc1 resulted in severe bleeding and premature death in mice (17). On the other hand, the *in vivo* role of Vkorc1l1 remains to be understood.

We have identified a *Vkorc1l1* mutant through a forward genetic screen for obesity-related loci in mice (23). In this report, we show that disruption of *Vkorc1l1* leads to defective adipogenesis associated with increased vitamin K_2 in preadipocytes. These results not only revealed a significant physiological function of *Vkorc1l1* but also expanded our knowledge regarding the initiation and progression of obesity.

Methods

Animals

All animal experiments were performed in accordance with guidelines from the Institutional Animal Care and Use Committee of the Institute of Developmental Biology and Molecular Medicine. Wild-type and mutant *FVB/NJ* mice were maintained in a specific pathogen-free facility with 12/12-hour light/dark cycles on normal chow diet or HFD. The piggyBac (PB) insertion (080508020-HRA) in *Vkorc1l1* was mapped in the first intron, with the PB targeted sequence TTAA at 130,446,713 bp of chromosome 5 (Ensembl version 53).

General and metabolic physiology

Mice were weighed and placed in a minispec nuclear magnetic resonance (NMR) instrument (Bruker, Billerica, Massachusetts) to measure the mass and ratio of body fat and lean compositions. Anal to nasal distance was measured as the body length. A fasting period of 8 hours was applied to 12-week-old mice prior to plasma hormone tests. Blood samples were then collected from the orbital sinus and analyzed with the Mouse Leptin and Insulin Ultrasensitive ELISA Kits (Crystal Chem, Inc., Elk Grove Village, Illinois).

For the intraperitoneal glucose tolerance test (IPGTT), 12-week-old mice were fasted for 16 hours before receiving an intraperitoneal injection of 20% glucose saline solution (2 g glucose per kilogram body weight). Tail vein blood was sampled at 0, 30, 60, and 120 minutes after injection. Area under curve of IPGTT data was calculated by Microsoft Excel (Redmond, Washington).

For triglyceride (TG) measurement, weighed adipose tissues were first homogenized in 500 μL of ddH_2O (prepared on site by a Millipore machine; Millipore, Burlington, Massachusetts) containing 5% NP-40 (Sangon Biotech, Shanghai, China). An aliquot of 10 μL 50-fold water diluted sample was then used to measure the TG concentration with a Triglyceride Assay Kit (EnzyChrom; BioAssay Systems, Hayward, California), such that the total amount of TG in adipose tissue could be calculated.

To determine the bone density, femurs were scanned by an Inveon CT (Siemens, Munich, Germany) and analyzed by the Inveon Research Workplace software.

Histology

Adipose tissues were fixed in ethanol and embedded in paraffin as described (24). Samples were sectioned at 10 μm and stained with hematoxylin and eosin.

Liver samples and subcutaneous adipose tissue of newborn mice were fixed in 4% paraformaldehyde, dehydrated in 30% sucrose at 4°C, prepared for 8-μm sections, and stained with hematoxylin and eosin as described (23).

Determination of adipocyte size and number

Individual adipocytes were isolated from adipose tissue by type I collagenase (Sangon Biotech) digestion as described (25). Adipocyte volumes were calculated with cell diameters measured by an EVOS XL Core Cell Imaging System (Thermo Fisher Scientific, Waltham, Massachusetts) and the NIH ImageJ software (Bethesda, Maryland) according to previous reports (26,27). The average adipocyte volume was calculated based on the data collected from three mice for each genotype, with approximately 200 adipocytes observed in each mouse.

Cell culture

Primary preadipocytes (stromal vascular fraction [SVF] cells) were isolated from inguinal WAT (iWAT) or interscapular BAT of P10 mice with type I collagenase (Sangon) as described (25). SVF cells and 3T3-L1 cells were cultured in DMEM/F12 medium containing 10% fetal bovine serum (FBS) (HyClone, GE Healthcare, Chicago, Illinois), 1% penicillin-streptomycin (Gibco, Gaithersburg, Maryland), and 1% L-glutamine (Gibco). SVF cells were differentiated by adding 10-μg/mL insulin (Sigma-Aldrich, St. Louis, Missouri), 1nM 3,3',5-triiodo-L-thyronine (T3; Sigma-Aldrich), and 125mM indomethacin (Sigma-Aldrich) for 8 days. 3T3-L1 cells were treated

for differentiation by 5-μg/mL insulin (Sigma-Aldrich), 250nM dexamethasone (Sigma-Aldrich), and 0.5mM IBMX (Sigma-Aldrich) on the first 2 days and by 5-μg/mL insulin for another 4 days. The differentiation medium was changed once every 2 days.

Vkorc1l1 small interfering RNA (siRNA) (5′-CCU CAG AAU CUU AAA CUG AUU TT-3′, GenePharma, Shanghai, China) and scramble siRNA (5′-UUC UCC GAA CGU GUC ACG UTT-3′, GenePharma) were transfected by Lipofectamin RNAiMax (Life Technologies, Carlsbad, California) according to the manufacturer's protocol. To test the knock efficiency, Western blot was performed 6 days after the transfection as previously described (28).

Lipolysis and lipogenesis analysis

To measure the basal level of lipolysis, four pieces of 50-mg perigonadal adipose tissue isolated from 6-hour-fasted mice were incubated at 37°C in 1 mL of OPTI-MEM (Gibco) containing 2% fatty-acid-free bovine serum albumin (BSA) for 2 hours. An aliquot of 10 μL medium was then used to measure the glycerol level with a Free Glycerol Assay Kit (Abcam, Cambridge, UK). To measure the stimulated level of lipolysis, 10μM Forskolin (Beyotime, Shanghai, China) was added in the OPTI-MEM fatty-acid-free BSA system for incubation.

For the quantification of lipogenesis, *in vitro* differentiated iWAT SVFs were cultured in OPTI-MEM containing 10% FBS with or without 25mM glucose for 2 days. Cells were homogenized in 1 mL of ddH_2O containing 5% NP-40. The TG content was measured in 10 μL fivefold water diluted sample by a Triglyceride Assay Kit (EnzyChrom).

Fluorescence activated cell sorting counting of primary preadipocytes

Isolated SVF cells were resuspended in ice-cold phosphate-buffered saline (PBS) with 5% FBS and stained with antimouse CD31 PE-Cyanine7 (catalog 25-0311; 1:100; eBioscience; Thermo Fisher Scientific, Waltham, Massachusetts), antimouse CD45 Alexa Fluor 700 (catalog 56-0451; 1:100; eBioscience), antimouse TER-119 APC-eFluor 780 (catalog 47-5921; 1:100; eBioscience), antimouse/rat CD29 APC (catalog 17-0291; 1:100; eBioscience), antimouse CD34 eFluor 450 (catalog 48-0341; 1:50; eBioscience), and antimouse Sca-1 FITC (catalog 11-5981; 1:100; eBioscience). Labeled samples were analyzed by Gallios flow cytometer (Beckman Coulter, Indianapolis, Indiana) and FlowJo software (FlowJo, LLC, Ashland, Oregon).

Oil Red O staining

Differentiated SVF or 3T3-L1 preadipocytes were fixed by 10% formalin at room temperature for 1 hour, incubated in 0.5% Oil Red O solution (dissolved in 60% isopropanol and 40% distilled water and filtered before use) for 30 minutes at 37°C, and extensively washed by distilled water before visualization. For quantitive experiments, Oil Red O was eluted by isopropanol and measured spectrophotometrically at 490 nm.

For differentiation experiments with vitamin K_1 or K_2, SVF cells were incubated with vitamin K_1 or K_2 throughout adipogenic induction and before Oil Red O staining. Relative differentiation rate was calculated by the ratio of quantified Oil Red O at 490 nm for each group treated with a different concentration of vitamin K_1 or K_2 to the solvent-treated group, which was set as 100%.

Frozen liver sections (8 μm) were fixed by 10% formalin at room temperature for 10 minutes, followed by a brief wash in 60% isopropanol aqueous solution. The samples were then stained in 0.5% Oil Red O solution followed by a brief wash in 60% isopropanol aqueous solution. Finally, the samples were briefly stained in hematoxylin solution and mounted with 80% glycerol aqueous solution.

Generation of Vkorc1l1 antibody

The Vkorc1l1 antibody was generated by ABclonal Biotechnology Co., Ltd (Woburn, Massachusetts). The antigen peptide is LVYLNEAWKRQLQPKED (amino acids 160-176 in the C-terminus). The antibody was produced by immunizing rats and affinity purified with the antigen.

Reverse transcription-polymerase chain reaction and Western blot

Total RNA was extracted with TRIzol (Invitrogen Corp., Carlsbad, California) and reverse transcribed (Takara Bio, Mountain View, California). Quantitative polymerase chain reaction (PCR) was performed using Brilliant QPCR Master Mix (Agilent Technologies, Santa Clara, California). 18s ribosomal RNA was used as an internal control.

Total protein was extracted from cultured cells with ice-cold radioimmunoprecipitation assay buffer and centrifuged at 15,000*g*. The supernatant was resolved by 10% sodium dodecyl sulfate polyacrylamide gel (SDS-PAGE), electrophoresis electrotransferred to a polyvinylidene difluoride membrane, and probed with rat anti-VKORC1L1 (1:200; generated by ABclonal), mouse anti-β-actin (catalog ab008-100; 1:2,000; Multisciences, Zhejiang, China), goat anti-rat IgG-HRP (catalog sc2006; 1:2,000; Santa Cruz Biotechnology, Dallas, Texas), or goat anti-mouse IgG-HRP (catalog sc2005, 1:2,000; Santa Cruz Biotechnology) antibodies. Densitometric quantification of VKORC1L1 protein level was determined by ImageJ and compared with β-actin (internal control) to determine the relative expression level.

Intracellular vitamin K_2 determination

Confluent SVF cells were treated with 16μM vitamin K_2 (menaquinone-4, Sigma-Aldrich) overnight. Cells were harvested, frozen, and thawed repeatedly by prechilled ethanol in liquid nitrogen and then sonicated. Cell lysates were dried *in vacuo*, dissolved in methanol, and resolved by high-performance liquid chromatography (HPLC) (Agilent SB-C18 column, 50*2.1 mm, 1.8 μm), with a mobile phase comprising methanol and isopropanol (50:50, v/v) at 0.4 mL/min. Vitamin K_2 signal peak was identified by comparing signals of wild-type SVF cells treated with 16μM vitamin K_2 with those of nontreated cells.

Statistics

Unless stated, data were presented as the mean ± SEM. An unpaired two-tailed Student *t* test was used to determine statistical significance.

Results

Disruption of *Vkorc1l1* causes lean phenotype in mice

The *Vkorc1l1* mutant was identified through a large-scale insertional mutagenesis project with the PB transposon (23). In this mutant, a

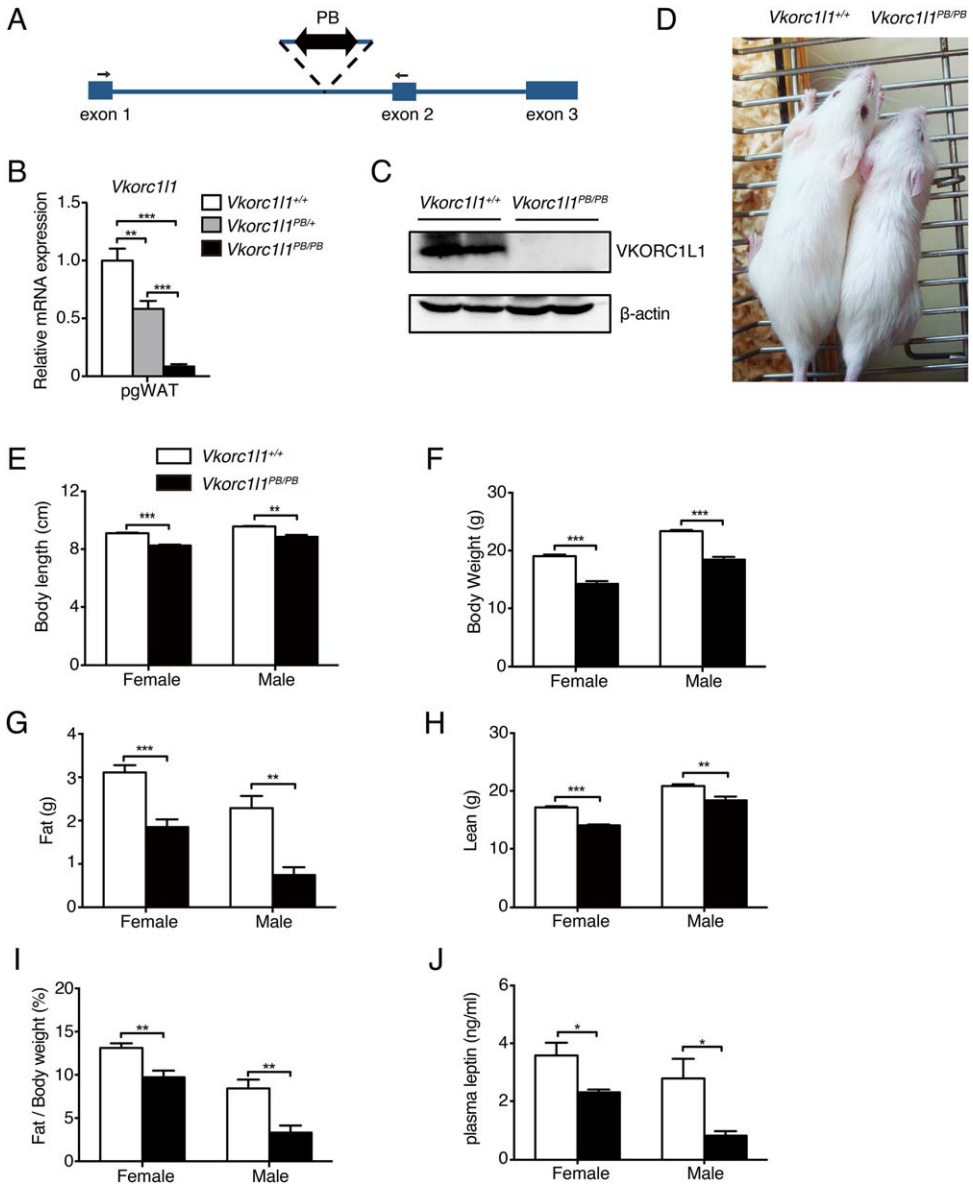

Figure 1 Disruption of *Vkorc1l1* in mice causes lean phenotypes. (**A**) A PB insertion in the second intron of *Vkorc1l1* diminishes gene expression, as measured by (**B**) quantitative RT-PCR against 18s rRNA in 6-week-old pgWAT ($n = 5\sim6$ for each group) or by (**C**) Western blot in P10 iWAT. Black arrows indicate binding sites of quantitative RT-PCR primers. (**D**) Dorsal view of a 5-month-old wild-type mouse and a *Vkorc1l1* mutant littermate. (**E,F**) Body length and body weight of 6-week-old mice ($n = 4$ for each group). (**G,H,I**) Fat mass, lean mass, and fat to body weight ratio of 12-week-old mice ($n = 6\sim11$ for each group). (**J**) Plasma leptin level of 12-week-old mice ($n = 5\sim8$ for each group). Data were presented as mean ± SEM. $^{*}P < 0.05$; $^{**}P < 0.01$; $^{***}P < 0.001$. [Color figure can be viewed at wileyonlinelibrary.com]

PB transposon was inserted in the first intron, which caused severely reduced gene expression (Figure 1A). In pgWAT, *Vkorc1l1* mRNA was decreased by approximately 50% in heterozygous ($Vkorc1l1^{PB/+}$) mice and essentially eliminated in the homozygotes ($Vkorc1l1^{PB/PB}$) (Figure 1B). In iWAT, VKORC1L1 proteins were undetectable in the homozygotes (Figure 1C). Severe reduction of *Vkorc1l1* mRNA was also detected in the BAT of $Vkorc1l1^{PB/PB}$ mice (Supporting Information Figure S1A). In contrast, mRNA levels of Vkorc1, the paralogue of Vkorc1l1, were not affected in mutant WAT or BAT (Supporting Information Figure S1B).

$Vkorc1l1^{PB/PB}$ animals are viable at birth (Supporting Information Figure S1C). They survive to adulthood with no obvious hemorrhage or other life-threatening abnormalities. However, homozygous mutants are apparently smaller than their wild-type littermates (Figure 1D), which may contribute to the smaller litter size of homozygous parents (Supporting Information Figure S1D). The average body length of $Vkorc1l1^{PB/PB}$ mice was approximately 10% less than that of the age-matched wild-type animals (Figure 1E). In addition, the average body weight of female and male $Vkorc1l1^{PB/PB}$ mice were 20.0% and 18.6% less than those of the wild-type littermates, respectively (Figure 1F).

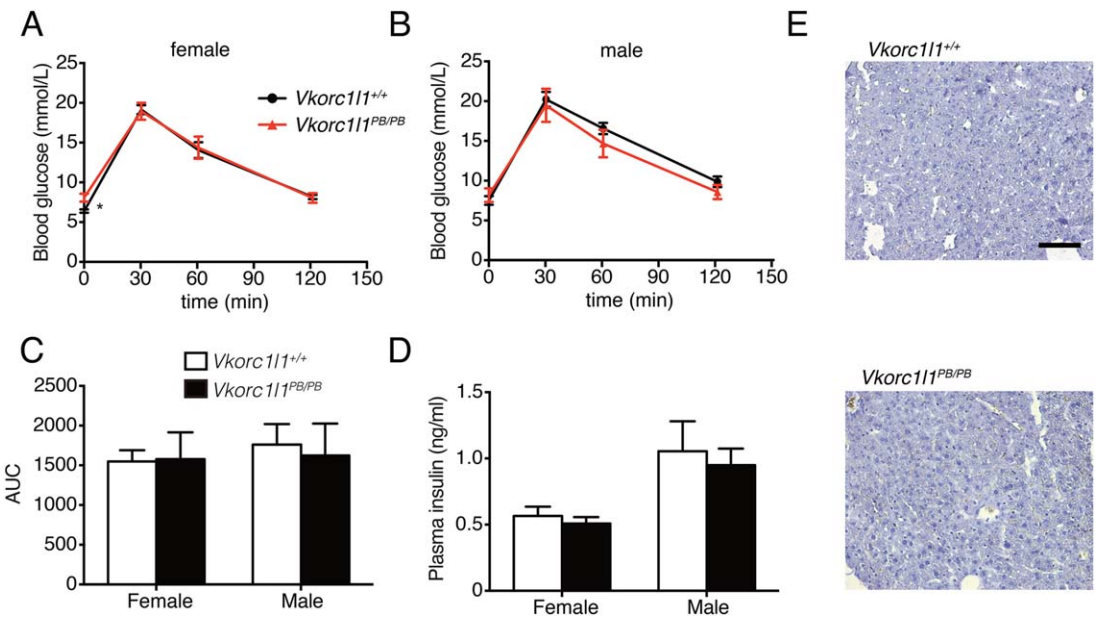

Figure 2 Absence of diabetes and fatty liver in *Vkorc1l1* mutants. (**A,B,C**) Glucose tolerance tests of 12-week-old mice (females, $n = 7\sim9$ for each group; males, $n = 6\sim11$ for each group). (**D**) Plasma insulin level of 12-week-old mice ($n = 6\sim10$ for each group). (**E**) Representative photographs of Oil Red O staining of 12-week-old liver section. Scale bar, 100 μm. Data were presented as mean ± SEM. $^*P < 0.05$. AUC, areas under the curve.

Meanwhile, the bone density of homozygous mutants was not affected (Supporting Information Figure S1E).

To determine whether the lower body weight of *Vkorc1l1*$^{PB/PB}$ mice resulted from less body fat, we measured their body compositions with NMR. Compared with those of the wild-type littermates, both fat and lean masses were reduced in *Vkorc1l1*$^{PB/PB}$ mice (Figure 1G-1H). In addition, the fat to body weight ratio was decreased by approximately 30% and 40% in female and male mutants, respectively (Figure 1I). Enzyme-linked immunosorbent assay (ELISA) analysis also revealed a significant decrease of plasma leptin levels in homozygous mutants (Figure 1J). These results confirmed loss of body fat in *Vkorc1l1*$^{PB/PB}$ animals.

Lipodystrophy is a rare genetic disorder characterized by loss of subcutaneous adipose tissue, which is often associated with insulin resistance, diabetes, and hepatic steatosis. Lipodystrophy has also been observed in *Agpat2* and *Seipin* mutant mice (29,30). To test whether this condition exists in *Vkorc1l1* mutants, we examined insulin sensitivity of *Vkorc1l1*$^{PB/PB}$ mice. When raised with normal chow diets, 12-week-old mutants and their wild-type littermates behaved comparably in the IPGTT (Figure 2A-2C). Their plasma insulin levels and hepatic fat accumulation conditions were also similar (Figure 2D-2E). When fed with HFD for 8 weeks, female mutants performed even better in IPGTT (Supporting Information Figure S1F). These results suggested that lipodysdrophy does not exist in *Vkorc1l1*$^{PB/PB}$ mice by this age.

To verify that the PB insertion was the causative mutation of these phenotypes, we crossed *Vkorc1l1*$^{PB/PB}$ animals with mice expressing the PB transposase to generate genetic revertants (*Vkorc1l1*$^{rev/rev}$) (23). Precise excision of the PB transposon in *Vkorc1l1*$^{rev/rev}$ mice was verified by sequencing (Supporting Information Figure S2A). In the revertants, *Vkorc1l1* transcription was recovered (Supporting Information Figure S2B). Mutant phenotypes such as alterations of the body weight, body length, and adipose tissue weight were no longer observed (Supporting Information Figure S2C-S2H). Taken together, these results indicated that disruption of *Vkorc1l1* led to the lean phenotype in mice.

Vkorc1l1 mutation affects white but not brown adipose

Both WAT and BAT may be affected in *Vkorc1l1*$^{PB/PB}$ mice to contribute to the observed lean phenotypes. To explore these possibilities, we examined iWAT, pgWAT, and retroperitoneal WAT (rWAT) as well as the interscapular BAT in 6-week-old *Vkorc1l1*$^{PB/PB}$ mice. Compared with those of the wild-type littermates, all mutant WATs exhibited smaller sizes (Figure 3A), lower weights, and lower tissue to body weight ratios (Figure 3B-3E). In fact, mutant WATs weighed only approximately half of the wild-type WATs. Detailed analysis of the pgWAT showed that compared with the wild-type adipose tissues, *Vkorc1l1*$^{PB/PB}$ adipose tissues had 27.8% fewer adipocytes in total (Figure 3F) and 18.2% less TG per gram of weight (Figure 3G). At the same time, the mutant adipocytes were 30.4% smaller than wild-type adipocytes (Figure 3H-3I). In contrast, the size of BAT and the BAT to body weight ratio of mutant mice were comparable with those of the wild-type littermates, although the weight of female BAT was 20.7% lighter (Figure 3A-3E). These results indicated that WATs were the major adipose depots affected by *Vkorc1l1* mutations in mice.

Vkorc1l1 mutation impairs preadipocyte differentiation

Induced beiging of WAT could stimulate the expression of thermogenic genes, which may in turn result in the lean phenotype (31).

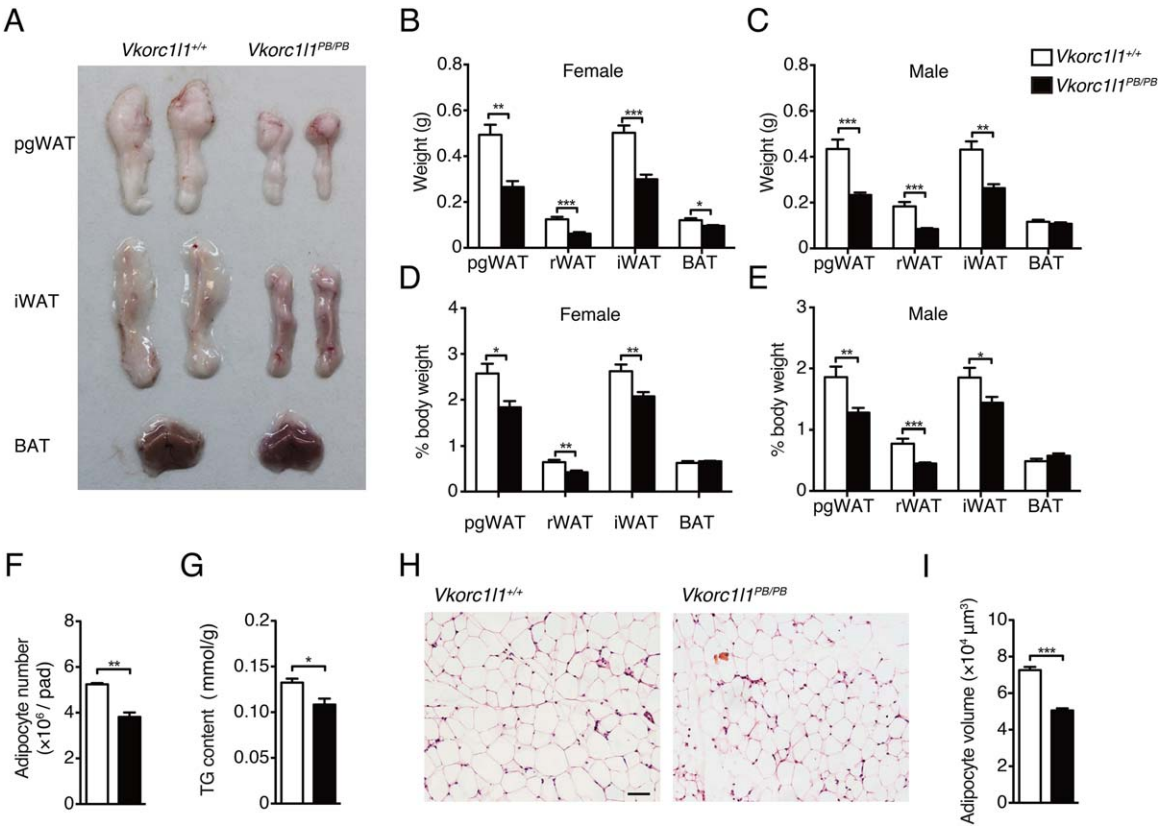

Figure 3 *Vkorc1l1* mutation affects white but not brown adipose. (**A**) Representative adipose depots from 6-week-old mice. (**B,C,D,E**) Absolute weight and fat to body weight ratios of pgWAT, rWAT, iWAT, and BAT depots from 6-week-old mice ($n = 5\sim6$ for each group). (**F**) Adipocyte number of pgWAT depots from 6-week-old mice ($n = 3$ for each group). (**G**) TG content in pgWAT depots from 6-week-old mice ($n = 3$ for each group). (**H**) Representative hematoxylin and eosin stainings of pgWAT and (**I**) quantification of adipocyte size in 6-week-old mice ($n = 3$ for each group). Scale bar, 50 μm. Data were presented as mean ± SEM. $^*P < 0.05$; $^{**}P < 0.01$; $^{***}P < 0.001$.

This is unlikely the case of *Vkorc1l1*$^{PB/PB}$ mutants because quantitative reverse transcription-polymerase chain reaction (RT-PCR) detected approximately 50% decreased expression of thermogenic genes *Ucp1* and *Pgc1a* in the iWAT of P10 homozygotes (Supporting Information Figure S3A). Defects in lipolysis and lipogenesis could also contribute to the lean phenotype in mice (32,33). However, no significant mRNA level alterations were observed for genes involved in lipolysis or lipogenesis upon the disruption of *Vkorc1l1* (Supporting Information Figure S3B-S3D). Consistent with this observation, we did not detect significant changes of glycerol release or TG accumulation in mutant tissues (Supporting Information Figure S3C-S3E). We thus followed adipose development, as smaller WATs in *Vkorc1l1*$^{PB/PB}$ mice could also be explained with defective tissue development. Examining mutant animals at birth, we found that the body weight of *Vkorc1l1*$^{PB/PB}$ mice was significantly decreased by 11.8% (Supporting Information Figure S3F). Necropsy analysis did not reveal gross malformations or weight alterations of organs such as BAT, liver, heart, or lung (Supporting Information Figure S3G), but it revealed a thinner cervical subcutaneous fat layer in newborn *Vkorc1l1*$^{PB/PB}$ mice (Figure 4A). NMR analysis also detected significantly reduced fat to body weight ratios in *Vkorc1l1*$^{PB/PB}$ mice at the age of 13 days (Supporting Information Figure S3H). These results strongly suggested defects in adipogenesis in *Vkorc1l1*$^{PB/PB}$ mice.

Adipogenic defects could result either from loss of preadipocytes (34) or from defective preadipocyte differentiation (35). We tested the former possibility by examining the expression of preadipocyte genes in adipose-derived regenerative and stem cells, which were defined collectively as the SVF (36). Quantitative RT-PCR detected increased expression of *Pdgfra, Pdgfrb*, and *NG2* in iWAT-derived SVF from 6-week-old *Vkorc1l1*$^{PB/PB}$ mice. Upregulation of *Pdgfra, Pdgfrb*, and *Vcam1* was also recognized in pgWAT-derived SVF from mutants at the same age. No decreased expression was observed for any of these preadipocyte genes (Figure 4B and Supporting Information Figure S3I). The number of preadipocytes (Ter119-:CD31-:CD45-:CD34+:CD29+:Sca1+) was increased by sixfold in iWAT-derived SVF from mutants (Figure 4C and Supporting Information Figure S4), as determined by flow cytometry. Thus, the decrease of preadipocyte population is unlikely the reason for adipogenic defects in *Vkorc1l1*$^{PB/PB}$ mice.

We then examined the differentiation of preadipocytes by measuring the expression of mature adipocyte genes, such as *Pparg2, Ap2,* adiponectin, and adipsin. Quantitative RT-PCR analysis of iWAT samples detected approximately 50% downregulation of these genes in *Vkorc1l1*$^{PB/PB}$ mice compared with those in wild-type littermates at the age of 10 days (Figure 4D). Induced differentiation of iWAT-derived SVF at the same age also resulted in aberrant differentiation.

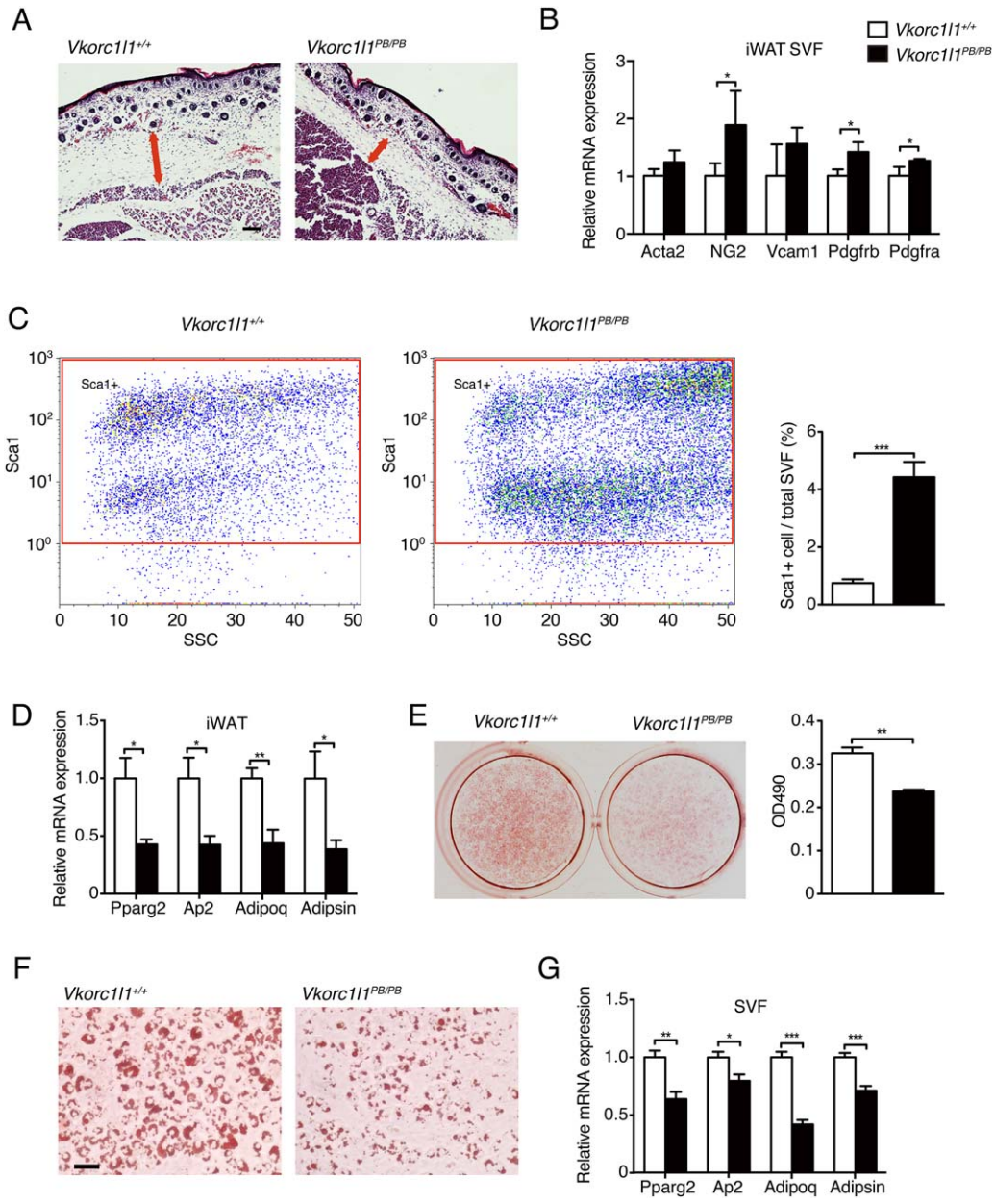

Figure 4 Defective adipose development in *Vkorc1l1* mutants. (**A**) Representative hematoxylin and eosin staining of P0 subcutaneous adipose tissue. The double-headed arrow indicates the fat layer. Scale bar, 100 μm. (**B**) Relative mRNA expression of preadipocyte marker genes in iWAT-derived SVF from 6-week-old mice ($n = 4$ for each group). (**C**) Representative dot plots showing fluorescence activated cell sorting staining and the number of preadipocytes (Ter119-:CD31-:CD45-:CD34+:CD29+:Sca1+) from 6-week-old mice ($n = 4$ for each group). (**D**) Relative mRNA expression of mature adipocyte marker genes from P10 iWAT ($n = 6$ for each group). (**E**) Global view and quantification of Oil Red O staining of differentiated iWAT SVF from P10 mice ($n = 3$ for each group). (**F**) Representative cell morphology and (**G**) relative mRNA expression of mature adipocyte marker genes of differentiated iWAT SVF from P10 mice ($n = 6$ for each group). Scale bar, 50 μm. Data were presented as mean ± SEM. $^*P < 0.05$; $^{**}P < 0.01$; $^{***}P < 0.001$.

After *in vitro* induction, Oil Red O staining detected a decreased number of lipid droplets with smaller sizes in *Vkorc1l1*$^{PB/PB}$ than in wild-type SVF cultures (Figure 4E-4F). Transcription of mature adipocyte genes was also significantly decreased (Figure 4G). Similar adipogenic defects could be observed in 3T3-L1 preadipocytes when *Vkorc1l1* expression was knocked down (Supporting Information Figure S3J-S3K). These results indicated that *Vkorc1l1* mutations led to defective preadipocyte differentiation.

Vitamin K_2 impairs adipogenesis and accumulates in *Vkorc1l1*-deficient preadipocytes

Previous studies have shown that induced adipogenesis in bone marrow cells could be inhibited by vitamin K_2 but not by vitamin K_1 (12). Considering the vitamin K epoxide reductase activity of Vkorc1l1 (22), we hypothesized that defective preadipocyte differentiation caused by *Vkorc1l1* mutations may be contributed by vitamin

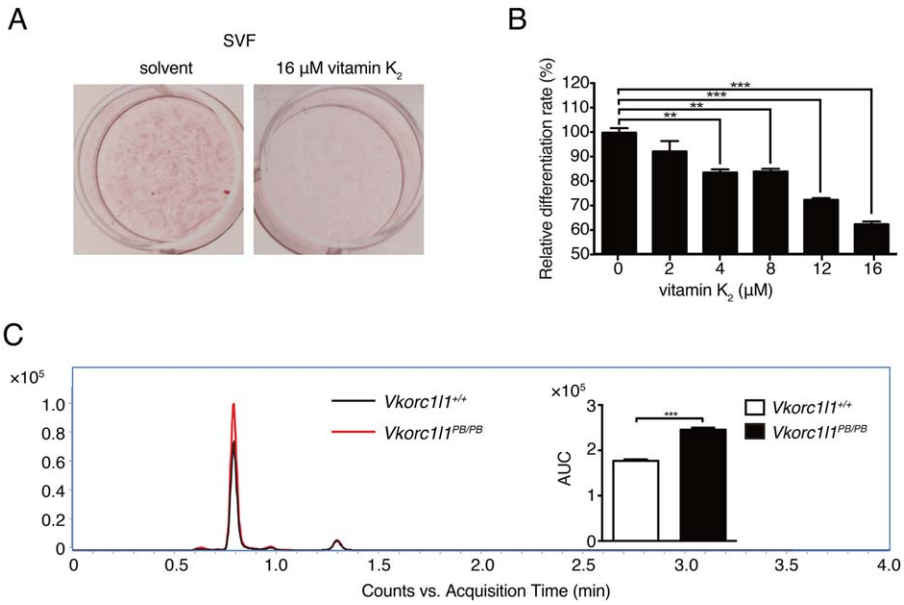

Figure 5 Vitamin K_2 impairs adipogenesis and accumulates in *Vkorc1l1*-deficient adipocytes. (**A**) Representative Oil Red O staining results of differentiated iWAT SVF from P10 mice; 16μM vitamin K_2 or the ethanol solvent were added in the medium, respectively. (**B**) Quantification of Oil Red O staining results of differentiated iWAT SVF from P10 mice with different concentrations of vitamin K_2 ($n = 3$ for each group). (**C**) Representative HPLC chromatogram of vitamin K_2 and area under the curve (AUC) of iWAT SVF from P10 mice ($n = 3$ for each group). Data were presented as mean ± SEM. $^{**}P < 0.01$; $^{***}P < 0.001$.

K_2 accumulation. To test this hypothesis, we first examined whether vitamin K_2 treatment could block preadipocyte differentiation. By incubating wild-type SVF cells with 16μM vitamin K_2 during adipogenic induction, we detected fewer adipocytes with Oil Red O staining and decreased expression of *Pparg2* (Figure 5A and Supporting Information Figure S5A). Quantitative comparison of OD490 value of the staining results further revealed that SVF cell differentiation was inhibited by vitamin K_2 in a dosage-dependent manner (Figure 5B). In contrast, vitamin K_1 did not affect SVF cell differentiation (Supporting Information Figure S5B). To further analyze whether the *Vkorc1l1* mutation induces vitamin K_2 accumulation, we examined intracellular vitamin K_2 levels by HPLC. We found $Vkorc1l1^{PB/PB}$ iWAT-derived SVF cells had 34.4% more vitamin K_2 than wild-type SVF cells (Figure 5C), indicating that vitamin K_2 metabolism was diminished by *Vkorc1l1* mutations. Intracellular vitamin K_2 was also increased in mutant BAT-derived SVF cells but to a lesser extent. Compared with wild-type BAT-derived SVF cells, $Vkorc1l1^{PB/PB}$ cells had 15.1% more vitamin K_2 (Supporting Information Figure S5C).

Discussion

In this study, we have reported a previously unknown function of *Vkorc1l1* in adipogenesis. This was supported by the fact that *Vkorc1l1* mutation led to underdeveloped WAT at birth and defective adipogenesis in cultured preadipocytes. Because of the increased number of preadipocytes and decreased adipocyte size in *Vkorc1l1* mutants, the observed adipogenic defects were not likely because of the loss of preadipocyte pool but more possibly caused by the accumulation of undifferentiated preadipocytes. BMDCs could also differentiate into adipocytes with a gender-specific pattern. However, considering that mutants of both genders showed severe defects in adipose tissues, it is unlikely that the defects of hematopoietic lineage cells were the main causes of the phenotypes of $Vkorc1l1^{PB/PB}$ mice.

Despite the severe WAT defects, lipodystrophic phenotypes such as insulin resistance, diabetes, and hepatic steatosis were not found in $Vkorc1l1^{PB/PB}$ mice. This could be due to the fact that WATs were not totally disrupted, such that the function of lipid storage partially remained in adipocytes to prevent ectopic fat deposition. Alternatively, the lipodystrophic phenotypes might occur in a later stage in the mutant life.

A previous report showed that vitamin K_1 could not inhibit the differentiation of preadipocytes *in vitro* (37). In our study, we have shown that vitamin K_2 but not vitamin K_1 suppressed adipogenesis of SVF cells. Consistent with our data, rats fed with either extra vitamin K_1 or K_2 displayed decreased body fat and serum TG (38). Considering that local tissues are likely capable of converting vitamin K_1 to vitamin K_2 in animals (15), these results support that vitamin K_2 plays the major role in impeding adipogenesis in mammals (14,37). As we have shown, vitamin K_2 could suppress the expression of *Pparg2*, which is a key regulator in promoting adipogenesis (Supporting Information Figure S5A). This could explain how vitamin K_2 suppresses adipogenesis. In addition, vitamin K_2 may regulate adipogenesis through PKA. It has been reported that vitamin K_2 could stimulate PKA, while hyperactive PKA could, in turn, suppress adipogenesis (19,39).

Although the organ weight of newborn pups and the bone density of adult mice were not affected by *Vkorc1l1* deficiency, reduced lean mass and body length were observed. These phenotypes suggested that vitamin K_2 accumulation may affect tissues in addition to WAT. Vitamin K_2 treatment could induce apoptosis in several cell

lines (40,41). A similar process may contribute to the growth defects in *Vkorc1l1*$^{PB/PB}$ mice. An overdose of vitamin K_1 may have similar effects, as it could be converted to vitamin K_2 *in vivo* (15).

Vkorc1 knockout mice displayed severe hemorrhagic phenotypes and died prematurely, while *Vkorc1l1*$^{PB/PB}$ mice were viable and fertile with a lean and small body (17). These differences in phenotypes indicated a significant difference between physiological functions of *Vkorc1* and *Vkorc1l1*, despite both possessing vitamin K epoxide reductase activity *in vitro*. In fact, these two paralogues appear to have significant differences in their structure and biochemical properties. Specifically, protein structure prediction suggested three transmembrane domains in Vkorc1 but four in Vkorc1l1 (22). Fluorescence protease protection assay suggested that the N-terminus of Vkorc1 faces cytoplasm and its C-terminus faces endoplasmic reticulum lumen, while both termini of Vkorc1l1 face cytoplasm (42). In addition, the amino acid sequence of Vkorc1 is less conserved than that of Vkorc1l1 (43,44). Moreover, previous data have indicated that Vkorc1, but not Vkorc1l1, is essential for vitamin-K-dependent carboxylation of osteocalcin (22,45). Our results have added another important function specifically associated with Vkorc1l1. The specific impact of Vkorc1l1 and vitamin K homeostasis on adipose development and their general impact on obesity and related metabolic disorders require future detailed assessment. O

Acknowledgments

We thank Xiaorong Huang, He Tan, Yanyan Nie, Liya Yang, Ying Yao, Boying Tan, Yanfeng Tan, Yueying Chen, and Yanqian Xia for animal care. We also thank Beibei Ying, Yufang Zheng, Ling V. Sun, Wufan Tao, Kejing Deng, Yuan Zhuang, and other Institute of Developmental Biology and Molecular Medicine members for valuable discussions.

References

1. Spiegelman BM, Flier JS. Adipogenesis and obesity: rounding out the big picture. *Cell* 1996;87:377-389.
2. Wu J, Bostrom P, Sparks LM, et al. Beige adipocytes are a distinct type of thermogenic fat cell in mouse and human. *Cell* 2012;150:366-376.
3. Houstek J, Kopecky J, Rychter Z, Soukup T. Uncoupling protein in embryonic brown adipose tissue--existence of nonthermogenic and thermogenic mitochondria. *Biochim Biophys Acta* 1988;935:19-25.
4. Birsoy K, Berry R, Wang T, et al. Analysis of gene networks in white adipose tissue development reveals a role for ets2 in adipogenesis. *Development* 2011;138:4709-4719.
5. Han J, Lee JE, Jin J, et al. The spatiotemporal development of adipose tissue. *Development* 2011;138:5027-5037.
6. Wang QA, Tao C, Gupta RK, Scherer PE. Tracking adipogenesis during white adipose tissue development, expansion and regeneration. *Nat Med* 2013;19:1338-1344.
7. Rigamonti A, Brennand K, Lau F, Cowan CA. Rapid cellular turnover in adipose tissue. *PLoS One* 2011;6:e17637. doi:10.1371/journal.pone.0017637
8. Spalding KL, Arner E, Westermark PO, et al. Dynamics of fat cell turnover in humans. *Nature* 2008;453:783-787.
9. Tang W, Zeve D, Suh JM, et al. White fat progenitor cells reside in the adipose vasculature. *Science* 2008;322:583-586.
10. Berry R, Rodeheffer MS. Characterization of the adipocyte cellular lineage in vivo. *Nat Cell Biol* 2013;15:302-308.
11. Cristancho AG, Lazar MA. Forming functional fat: a growing understanding of adipocyte differentiation. *Nat Rev Mol Cell Biol* 2011;12:722-734.
12. Takeuchi Y, Suzawa M, Fukumoto S, Fujita T. Vitamin k(2) inhibits adipogenesis, osteoclastogenesis, and odf/rank ligand expression in murine bone marrow cell cultures. *Bone* 2000;27:769-776.
13. Majka SM, Fox KE, Psilas JC, et al. De novo generation of white adipocytes from the myeloid lineage via mesenchymal intermediates is age, adipose depot, and gender specific. *Proc Natl Acad Sci U S A* 2010;107:14781-14786.
14. Shearer MJ, Newman P. Metabolism and cell biology of vitamin K. *Thromb Haemost* 2008;100:530-547.
15. Okano T, Shimomura Y, Yamane M, et al. Conversion of phylloquinone (vitamin K1) into menaquinone-4 (vitamin K2) in mice: two possible routes for menaquinone-4 accumulation in cerebra of mice. *J Biol Chem* 2008;283:11270-11279.
16. Al-Terkait F, Charalambous H. Severe coagulopathy secondary to vitamin K deficiency in patient with small-bowel resection and rectal cancer. *Lancet Oncol* 2006;7:188. doi: 10.1016/S1470-2045(06)70583-6
17. Spohn G, Kleinridders A, Wunderlich FT, et al. Vkorc1 deficiency in mice causes early postnatal lethality due to severe bleeding. *Thromb Haemost* 2009;101:1044-1150.
18. Misasi S, Martini G, Paoletti O, et al. Vkorc1 and cyp2c9 polymorphisms related to adverse events in case-control cohort of anticoagulated patients. *Medicine (Baltimore)* 2016;95:e5451. doi:10.1097/MD.0000000000005451
19. Ichikawa T, Horie-Inoue K, Ikeda K, Blumberg B, Inoue S. Vitamin k2 induces phosphorylation of protein kinase a and expression of novel target genes in osteoblastic cells. *J Mol Endocrinol* 2007;39:239-247.
20. Tabb MM, Sun A, Zhou C, et al. Vitamin k2 regulation of bone homeostasis is mediated by the steroid and xenobiotic receptor sxr. *J Biol Chem* 2003;278:43919-43927.
21. Stafford DW. The vitamin K cycle. *J Thromb Haemost* 2005;3:1873-1878.
22. Westhofen P, Watzka M, Marinova M, et al. Human vitamin K 2,3-epoxide reductase complex subunit 1-like 1 (vkorc1l1) mediates vitamin K-dependent intracellular antioxidant function. *J Biol Chem* 2011;286:15085-15094.
23. Cui J, Ding Y, Chen S, et al. Disruption of gpr45 causes reduced hypothalamic pomc expression and obesity. *J Clin Invest* 2016;126:3192-3206.
24. Krishnamurthy H, Babu PS, Morales CR, Sairam MR. Delay in sexual maturity of the follicle-stimulating hormone receptor knockout male mouse. *Biol Reprod* 2001;65:522-531.
25. Prunet-Marcassus B, Cousin B, Caton D, Andre M, Penicaud L, Casteilla L. From heterogeneity to plasticity in adipose tissues: site-specific differences. *Exp Cell Res* 2006;312:727-736.
26. Goldrick RB. Morphological changes in the adipocyte during fat deposition and mobilization. *Am J Physiol* 1967;212:777-782.
27. Jo J, Gavrilova O, Pack S, et al. Hypertrophy and/or hyperplasia: dynamics of adipose tissue growth. *PLoS Comput Biol* 2009;5:e1000324. doi:10.1371/journal.pcbi.1000324
28. Zhu X, Xie S, Xu T, Wu X, Han M. Rasal2 deficiency reduces adipogenesis and occurrence of obesity-related disorders. *Mol Metab* 2017;6:494-502.
29. Cortes VA, Curtis DE, Sukumaran S, et al. Molecular mechanisms of hepatic steatosis and insulin resistance in the AGPAT2-deficient mouse model of congenital generalized lipodystrophy. *Cell Metab* 2009;9:165-176.
30. Cui X, Wang Y, Tang Y, et al. Seipin ablation in mice results in severe generalized lipodystrophy. *Hum Mol Genet* 2011;20:3022-3030.
31. Seale P, Conroe HM, Estall J, et al. Prdm16 determines the thermogenic program of subcutaneous white adipose tissue in mice. *J Clin Invest* 2011;121:96-105.
32. Miyazaki M, Flowers MT, Sampath H, et al. Hepatic stearoyl-coa desaturase-1 deficiency protects mice from carbohydrate-induced adiposity and hepatic steatosis. *Cell Metab* 2007;6:484-496.
33. Wang SP, Laurin N, Himms-Hagen J, et al. The adipose tissue phenotype of hormone-sensitive lipase deficiency in mice. *Obes Res* 2001;9:119-128.
34. Carnevalli LS, Masuda K, Frigerio F, et al. S6k1 plays a critical role in early adipocyte differentiation. *Dev Cell* 2010;18:763-774.
35. Birsoy K, Chen Z, Friedman J. Transcriptional regulation of adipogenesis by klf4. *Cell Metab* 2008;7:339-347.
36. Rodbell M. Metabolism of isolated fat cells. I. Effects of hormones on glucose metabolism and lipolysis. *J Biol Chem* 1964;239:375-380.
37. Kawada T, Aoki N, Kamei Y, Maeshige K, Nishiu S, Sugimoto E. Comparative investigation of vitamins and their analogues on terminal differentiation, from preadipocytes to adipocytes, of 3t3-l1 cells. *Comp Biochem Physiol A Comp Physiol* 1990;96:323-326.
38. Sogabe N, Maruyama R, Baba O, Hosoi T, Goseki-Sone M. Effects of long-term vitamin K(1) (phylloquinone) or vitamin K(2) (menaquinone-4) supplementation on body composition and serum parameters in rats. *Bone* 2011;48:1036-1042.
39. Li F, Wang D, Zhou Y, et al. Protein kinase a suppresses the differentiation of 3t3-l1 preadipocytes. *Cell Res* 2008;18:311-323.
40. Tokita H, Tsuchida A, Miyazawa K, et al. Vitamin k2-induced antitumor effects via cell-cycle arrest and apoptosis in gastric cancer cell lines. *Int J Mol Med* 2006;17:235-243.
41. Nishimaki J, Miyazawa K, Yaguchi M, et al. Vitamin k2 induces apoptosis of a novel cell line established from a patient with myelodysplastic syndrome in blastic transformation. *Leukemia* 1999;13:1399-1405.
42. Tie JK, Jin DY, Stafford DW. Conserved loop cysteines of vitamin K epoxide reductase complex subunit 1-like 1 (vkorc1l1) are involved in its active site regeneration. *J Biol Chem* 2014;289:9396-9407.
43. Oldenburg J, Watzka M, Bevans CG. Vkorc1 and vkorc1l1: why do vertebrates have two vitamin K 2,3-epoxide reductases? *Nutrients* 2015;7:6250-6280.
44. Robertson HM. Genes encoding vitamin-K epoxide reductase are present in drosophila and trypanosomatid protists. *Genetics* 2004;168:1077-1080.
45. Ferron M, Lacombe J, Germain A, Oury F, Karsenty G. Ggcx and vkorc1 inhibit osteocalcin endocrine functions. *J Cell Biol* 2015;208:761-776.